Environmental Earth Sciences (2024) 83:322
https://doi.org/10.1007/s12665-024-11603-4

ORIGINAL ARTICLE

Some correlations between the river regime and land cover changes caused by climate change in the Selenge River Basin, Mongolia

Erdenebayar Bavuu[1,2] · Batsuren Dorjsuren[1,5] · Davaa Gombo[2] · Juanle Wang[3] · Erdenetsetseg Sugar[1] · Bolorjargal Ganzorig[2] · Oyunchimeg Namsrai[1] · Adiyasuren Tserenjargal[4] · Shuxing Xu[3] · Yating Shao[3] · Altansukh Ochir[1]

Received: 28 November 2023 / Accepted: 9 April 2024 / Published online: 10 May 2024

Abstract

The Selenge River Basin is one of the major tributaries of Lake Baikal, one of the world's freshwater resources, and is a sensitive region to climate change, and is also an important China–Mongolia–Russia economic corridor basin. Therefore, studying the relationship between the eco-hydrological processes of this basin and its land cover changes is important for sustainability and environmental protection. In this research, trend analysis was used to determine water and climate changes, and satellite data and statistical analysis were used to calculate spatial and temporal changes in land cover. Based on the research findings, the flow of the Selenge River has exhibited fluctuations ranging from 125.2 to 576.3 m^3/s over the past three decades, with a discernible downward trend observed in the basin area or at the Zuunburen hydrological station. This decline can be attributed to the combined effects of climate change and human activity. During the last 30 years of climate change in the Selenge River basin, the average annual air temperature has increased by 2.4 °C. The average total annual precipitation of the basin ranges from 200 to 400 mm, and the precipitation fluctuation is relatively small, and in recent years, less than average precipitation has fallen. In the basin, the air temperature has experienced an annual increase of 0.09 °C, attributable to natural climatic factors. Additionally, there has been a reduction in both precipitation levels and river flow within the basin, while significant alterations have occurred in the extent of water bodies and wetlands within the land cover. In this region, studies show that changes in eco-hydrological processes significantly impact changes in land cover.

Keywords Climate change · Land cover change · Mann–Kendall test · River discharge · Selenge River Basin

Introduction

Scientists concur that the Earth is undergoing a warming trend (McCright et al. 2013; Masson-Delmotte et al. 2021). Over the past century, there has been an observed rise in the mean atmospheric temperature of approximately 0.6 °C (Hansen et al. 2001). The consensus among the scientific community posits that both anthropogenic influences and natural climatic variability contribute to global warming. Consequently, it is anticipated that global mean atmospheric temperatures will ascend within the range of 1.0–3.5 °C by the year 2100 (Førland et al. 2011; Millar et al. 2017). Heterogeneity characterizes temperature variations across different regions worldwide (Cianconi et al. 2020).

Mongolia exhibits an extreme continental climate owing to its positioning in the northern part of Central Asia. Situated within the transitional belt linking the expansive Siberian taiga and the arid Central Asian desert, the region experiences protracted and arid winters alongside brief summers (Batima et al. 2008; Yembuu and Yembuu 2021). Since the 1940s, Mongolia has observed a rise in its average temperature by approximately 1.7 °C. Projections indicate that over the forthcoming 80 years, summer temperatures is anticipated to increase by 2 °C, while winter temperatures are forecasted to elevate by 1 °C (Сато et al. 2007). Over the preceding 6 decades, Mongolian glaciers have experienced a reduction in size ranging from 10 to 30% (Konya et al. 2013). In Mongolia, variations in climatic and geographical parameters delineate distinct natural zones, each susceptible to differential from climate change. Projections suggest a diminution in precipitation and soil moisture across the majority of taiga forest regions in central and northern Mongolia (Sato et al. 2008).

Extended author information available on the last page of the article

Mongolia's territory and its river basins are devoid of flowing rivers, owing to its positioning exclusively within the Arctic and Pacific Oceans, as well as the Central Asian Land Locked basin. The Selenge River, encompassing an area of 447,060 km^2, serves as the principal outlet for Baigal Lake (Davaa 2015). Of its total area, 20.2% lies within the Arctic Ocean basin, 16.0% within the Pacific Ocean basin, and 63.8% within the Central Asian Land Locked Basin.

These factors encompass its pivotal role as the primary water source and watershed for Lake Baikal, its strategic significance within the Sino-Mongolian-Russian Economic Corridor, and its status as a critical development area for Lake Baikal region (Dorjsuren et al. 2018; Zorigt et al. 2019). Changes in land use and land cover within the basin exerts direct influence on water resources throughout the entire region (Batdelger et al. 2022; Ren et al. 2022; Karthe et al. 2017). The Selenge River Basin exhibits a diverse array of land use types, encompassing grazing, mining, forestry, and agricultural activities (Stubblefield et al. 2005).

Given that the Selenge River basin contributes over 60% of Mongolia's agricultural yield, intensive agricultural practices wield a substantial influence on the production of agricultural commodities within the basin (Цыренова 2011). The impact of land degradation resulting from mining activities has resulted in a limited extent of affected area within the Selenge River Basin, primarily due to the predominant land uses of cultivation and pasture (Timofeev and Kosheleva 2017). A significant expansion of Mongolia's agricultural land has occurred in the Selenge River Basin, in the northern part of the country. Recent observations within the basin indicate notable alterations in ecosystems and water resources attributed to climate change and anthropogenic activities, underscoring the necessity of conducting comprehensive research in this area. Recent studies highlight the importance of Evaporation Change, Land Use, and Land Cover Change analyses as primary tools for elucidating the impacts of climate change and eco-hydrological processes within the basin, facilitating adaptation strategies and effective management practices (Dorjsuren et al. 2018, 2021).

The primary objective of this study is to conduct an in-depth examination of the interplay between the river regime, water resources, climate change, and land cover dynamics within the Selenge River basin. To achieve this purpose, the following actions are proposed: (i) delineating historical trends in hydrological and meteorological parameters, (ii) assessing alterations in land cover, specifically focusing on variations in water bodies and wetlands, and (iii) quantifying the extent to which changes in land cover and climate influence river regimes and water resources, as well as exploring the interdependencies among these variables.

Materials and methods

Study area

The Selenge River is in Mongolia, in the northern part of Central Asia (51°52′–109°20′ N, 46°25'–96°48′ W) (Ma et al. 2003; Dorjsuren et al. 2018). Lake Baikal is also located here, and its catchment area is 573,478 km^2 (Гармаев and Доржготов 2010). Nevertheless, the Selenge River has a basin area of 295,694 km^2, an average height of 1598 m, and a total length of 1500 km, of which 1095 km are in Mongolia. A total of 9 sub-basins are included in the basin: Tuul, Orkhon, e.g, Ider, Khanui, Kharaa, Eroo, Delgermoron, and Chuluut (Fig. 1). The average annual air temperature for Mongolia's Selenge River basin is 0.83 °C. The average air temperature has significantly increased in the past 60 years. The mean temperature is 16–18 °C in July and − 16 to − 22 °C in January. In Mongolia's Selenga river basin, precipitation varies both in time scale and space scale. Annual mean precipitation is 300–400 mm/year in the Khangai, Khentein, and Huvsgul mountainous regions and 150–250 mm/year in the steppe and river valleys (Dorjsuren et al. 2018).

Therefore, a total of 8 hydrological and 7 meteorological stations were selected and used in this research work: Tuul–Ulaanbaatar station on the Tuul River, Eroo–Eroo station on the Eroo River, Orkho–Kharkhorin station on the Orkhon River, Urdtamir–Tsetserleg station, Orkhon–Orkhon station, Chuluut–Chuluut station on the Chuluut River, Ider–Ider station on the Ider River, and Delgermoron station on the Delgermoron River, Eg–Erdenebulgan station on the Delgermoron and Eg Rivers, and Selenge–Zuunburen station on the Selenge River. As shown in Fig. 1, seven meteorological stations and eight hydrological stations were used in this study. The selection of hydrological and meteorological stations within the Selenge River basin in Mongolia was guided by rigorous criteria, including but not limited to the following factors: (1) Spatial distribution across the basin to ensure comprehensive coverage, (2) Consideration of the operational history and reliability of each station, as indicated by the duration of data records, and (3) Availability of existing hydrological and meteorological infrastructure to facilitate data collection and monitoring efforts (Dorjsuren et al. 2018, 2021).

Data sources

The study employed a robust dataset encompassing climate and river discharge measurements spanning from 1990 to 2020, sourced from meticulously maintained

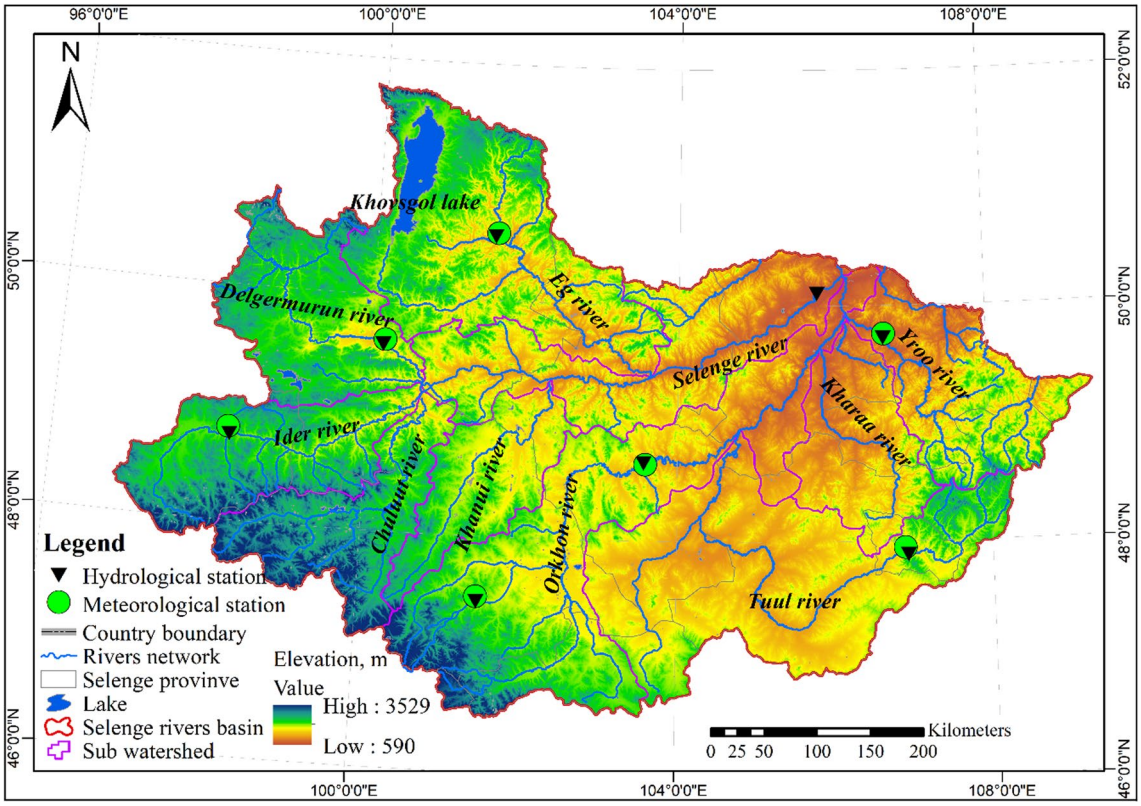

Fig. 1 Location of hydrological and meteorological stations in the Selenge River basin

hydro-meteorological stations and gauges strategically positioned at key locations including Ulaanbaatar, Tsetserleg, Orkhon, Baruunkharaa, Moron, Tsagaan-Uur, and Tosontsengel sites. Specifically, temperature, precipitation, and hydrological data of the Selenge River basin in Mongolia were obtained from the Information and Research Institute of Meteorology, Hydrology Environmental (IRIMHE) Analysis database (http://irimhe.namem.gov.mn/).

Complementing this dataset, land cover data from the period 1990–2020 were obtained from esteemed National Geomatics Center of China. This dataset boasts a spatial resolution of 30 m and is characterized by observations captured at 10-year intervals. Such a comprehensive dataset facilitated rigorous scientific analysis and modeling endeavors, enabling an in-depth exploration of the interplay between climate dynamics, river runoff patterns, and land cover transformations within the study region.

At 10-year intervals between 1990 and 2020, Landsat Thematic Mapper (TM) and Landsat Enhanced and Thematic Mapper (ETM+) satellite data with 30-m spatial resolution were used to calculate land cover changes. (http://landsat.usgs.gov/). It was based on the Global Land Cover Database (GlobeLand30) released by the China National Geomatics Center in 2014.

Methods

Changes in river flow are calculated independently by expressing changes in flow over time (McClelland et al. 2006). A Mann–Kendall (MK) method was used to detect trends in river flows and climate changes the purpose of this method is to assess changes in hydrological flows and to examine trends in those changes. A Mann–Kendall (MK) method was used to verify the results, and ITAM and Sen's slope calculation methods were used to confirm them. Time series data were analyzed statistically and comparisons were made between seasonal, annual, and multi-year averages. Climate and river flow time series data were evaluated using MK, ITAM, and Sen's slope calculations, and results were

developed at 5%, 10%, and 1% significance levels. Within the realm of eco-hydrological investigations concerning the temporal and spatial dynamics of water–climate, the utilization of trend analysis and land cover change methodologies has been recurrently documented to elucidate their intricate interdependencies. In the present study, trend analysis was judiciously employed to discern and quantify the temporal alterations in water–climate dynamics, while land cover change methodologies were applied to estimate spatiotemporal variations therein. This methodological framework facilitated a comprehensive examination of the nuanced relationships between water–climate fluctuations and land cover transformations, thereby enriching our understanding of eco-hydrological processes at both temporal and spatial scales. This study followed the methodological scheme shown in (Fig. 2).

Mann–Kendall (MK) test method

The Mann–Kendall (MK) method shows trends in statistical correlations. A statistical correlation depends on the size of the data, the sample size, and the variance of the series. Moreover, Mann–Kendall (MK) trends are a way to identify outliers in a data series because the MK test statistic is dependent on positive and negative signs (Dorjsuren et al. 2021; Asfaw et al. 2018; Gedefaw et al. 2018a). The purpose of this study was to identify changes and trends in river flow. Trends in river flows were compared with long-term climate statistics. Mann–Kendall (MK) estimates correlation using all values. Mann–Kendall (MK) statistic formula (S) is calculated as follows:

$$S = \sum_{(i=1)}^{(n-1)} \sum_{(j=i+1)}^{n} sgn(x_j - x_i) \quad (1)$$

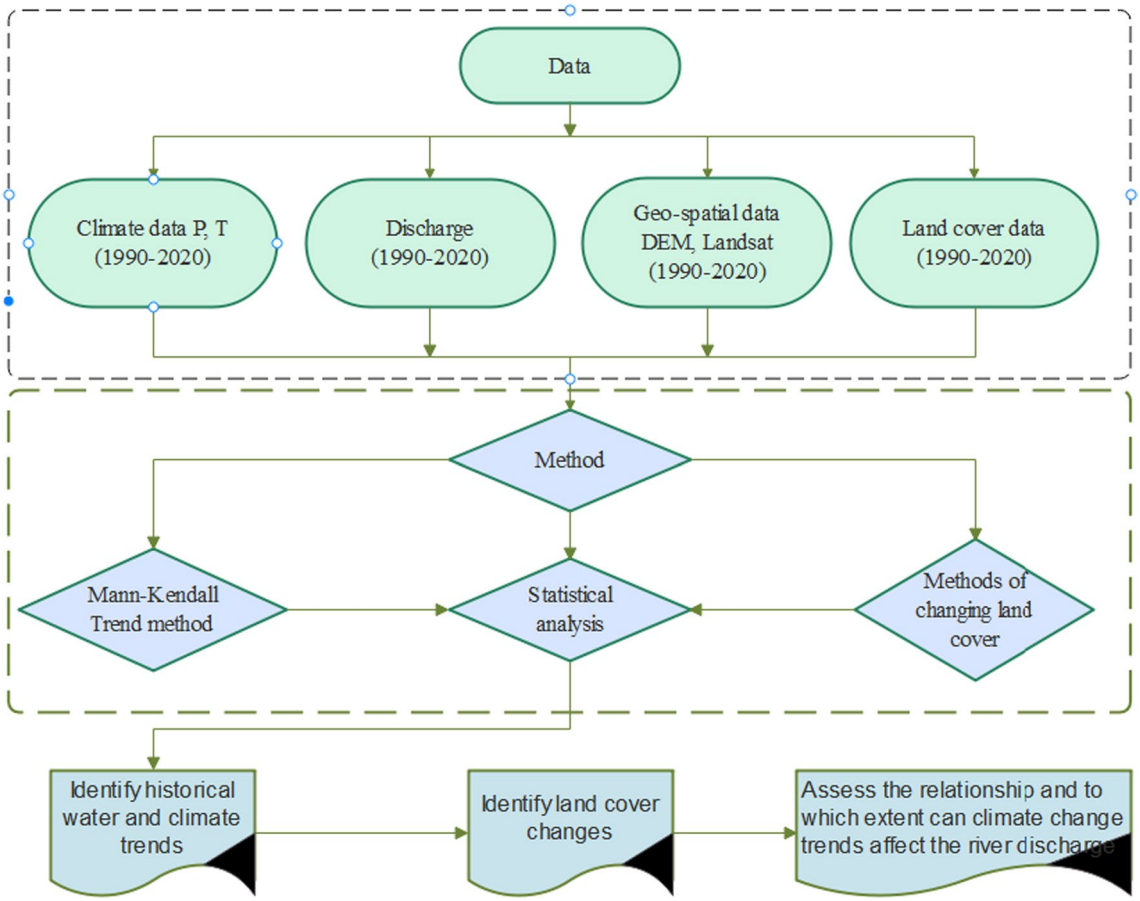

Fig. 2 A methodology for calculating trends in river flows in the Selenge River basin

The trend test is applied to x_i $(i = 1, 2, \ldots n-1)$ and $x_j (j = i+1, 2, \ldots n)$. The value of each x_i is used as a reference point to compare with the value of x_j, which is given as

$$sgn(x_j - x_i) = \begin{cases} +1 \text{ if } (x_j - x_i) > 0 \\ 0 \text{ if } (x_j - x_i) = 0 \\ -1 \text{ if } (x_j - x_i) < 0 \end{cases}, \quad (2)$$

where x_j and x_i represent values in periods j and i, respectively. When the number of data series is greater than or equal to ten ($n \geq 10$), the Mann–Kendall (MK) method defines the mean value using a normal distribution as follows: $E(S) = 0$. The variation of the time series Var(S) is calculated as follows (Ma et al. 2014):

$$E(S) = 0, \quad (3)$$

$$Var(S) = \frac{n(n-1)(2n+5) - \sum_{k=1}^{m} t_k(t_k-1)(2t_k+5)}{18}, \quad (4)$$

where m is the number of the tied groups in the time series, and t_k is the number of ties in the k_{th} tied group. The test statistics Z is as follows:

$$Z = \begin{cases} \frac{s-1}{\delta} \text{ if } S > 0 \\ 0, \text{ if } S = 0 \\ \frac{s+1}{\delta} \text{ if } S < 0 \end{cases}. \quad (5)$$

When Z is greater than zero, it indicates an increasing trend and when Z is less than zero, it is a decreased trend. In time sequence, the statistics are defined independently (Demberel et al. 2023; Enkhbold et al. 2022):

$$UF_k = \frac{d_k - E(d_k)}{\sqrt{var(d_k)}} (k = 1, 2, \ldots, n). \quad (6)$$

Then, the time sequence is arranged in reverse order. According to the equation calculation, while making (Erdenejargal et al. 2021; Girma et al. 2023):

$$UB_k = -UF_k, \quad (7)$$

$$K = n + 1 - k. \quad (8)$$

In this, UB_k and UF_k when expressing the statistical series, the time sequence is also expressed in reverse order. In this way, the validity of the results of the research will be confirmed. Inverse sequences produce linear curves that are symmetric with primary sequences. It indicates that there is an error in the time series data if a symmetrical curve does not appear (Wu et al. 2017).

Innovative trend analysis method (ITAM)

Innovating Trend Analysis Method (ITAM) is a method for identifying hydrological conditions and comparing its accuracy with Mann–Kendall (MK) results (Wu and Qian 2017; Cui et al. 2017). Defining the indicator is as follows:

$$\Phi = \frac{1}{n} \sum_{i=1}^{n} \frac{10(x_j - x_i)}{\mu}, \quad (9)$$

where Φ= trend indicator, n = number of observations on the subseries, x_i = data series in the half subseries class, x_j = data series in the half subseries part and μ = mean of data series in the first half subseries part.

Sen's slope estimator test

The slope calculation method determines the amount of water flowing (Gedefaw et al. 2018a; Gedefaw et al. 2018b). A slope Q_i is defined as follows:

$$Q_i = \frac{x_j - x_k}{j - k}, \text{for } i = 1, 2, \ldots N, \quad (10)$$

where x_j and x_k are data points at time j and $(j > k)$, respectively. When there is only a single datum at each time point, then N is calculated as $N = \frac{n(n-1)}{2}$; where 'n' is the number of time periods. However, if the number of data in each year is many, then $N < \frac{n(n-1)}{2}$; n total number of observations. Then N value of the slope estimator is arranged from the smallest to the biggest. Then, the median of slope (β) is computed as

$$\beta = \begin{cases} Q[(N+1)/2] \, when \, N \, is \, odd \\ Q[(N/2) + Q(N+2)/(2)/(2)] \, when \, N \, is \, even \end{cases}. \quad (11)$$

Land cover methods

The change in land cover over time was determined by comparing the first and subsequent periods (Dorjsuren et al. 2018).

$$CA = TA(t_1) - TA(t_2) \tag{12}$$

$$CE = \left[CA/TA(t_1)\right] * 100 \tag{13}$$

where $TA = total\ area$, $CA = changed\ area$, $CE = the\ extent\ of\ change$, $t_1 = begining\ time, t_2 = ending\ time$

$$K = P(A) - P(E)/1 - P(E) \tag{14}$$

where K is the kappa coefficient, P(A) is the number of times the K raters agree, and P(E) is the number of times the K rates are expected to agree only by chance.

Statistical analysis

Linear Regression: A technique used to identify trends over time by comparing climate trends with river discharges (Gedefaw et al. 2018a; Chonokhuu et al. 2019). The regression parameter a and its coefficient b are estimated using the least squares method and calculated using the equation below. Where:

$$b = \frac{\sum_{i=1}^{n}\left(x_i - \bar{x}\right)\left(y_i - \bar{y}\right)}{\sum_{i=1}^{n}\left(x_i - \bar{x}\right)^2}, \tag{15}$$

where $x = \frac{1}{N}\sum_{i=1}^{n} x_i y = \frac{1}{N}\sum_{i=1}^{n} y_i$ if $b > 0$, this indicates the climate factor tends to increase, and that when $b < 0$, it tends to decrease.

Correlation coefficient: This method was used to calculate the effect of hydro climate on land cover changes in the Selenge River Basin. The correlation coefficient method was used to calculate it.

$$r = \frac{\sum(x - \bar{x})(y - \bar{y})}{\sqrt{\left(\sum\left(x - \bar{x}\right)^2 \sum(y - \bar{y})^{-2}\right.}} \tag{16}$$

where: y_i- correlation coefficient, xi- A variable for exceptions, x- the mean of the exception variable, y_i-variables, y_i- the mean of the variables. In this equation, x and y are the averages of the sample values, $rxy > 0$ indicates a positive correlation and $rxy < 0$ indicates a negative correlation (Gedefaw et al. 2018b).

Results

Climate change and water trend

Analysis of air temperature

Using the Mann–Kendall method, we analyzed the average air temperature at seven stations in the Selenge River basin over the last 31 years. In Ulaanbaatar city, it has continuously increased since 1994, with a significant rise observed since 2015." The highest value of Z was found in this area ($Z = 4.50$). Moreover, the average air temperature changes in Tsetserleg ($Z = 2.27$), and Tosontsengel ($Z = 2.88$), as well as the average change in air temperature at these stations show a stable growth trend. In other regions, however, the average change in air temperature was small ($Z = -0.26$ to 1.95), or close to the average for many years. Since 1994, the area's average temperature has increased continuously ($Z = 1.77$) (Fig. 3).

The results of calculating the annual average air temperature of the basin using MK, ITAM, and Sen's slope calculation method are shown in Table 1. Between 1990 and 2005, average air temperatures in the Selenge River basin decreased, but in recent years, an increasing trend has been observed at all stations.

Analysis of precipitation

The Mann–Kendall method was used to analyze precipitation data from 7 stations in the Selenge river basin over the last 31 years. The total annual precipitation changes for the Tsagaan-Uur area from 1990 to 2010 was ($Z = 2.68$), which means that some years were wetter than average. However, in the Orkhon and Baruunkharaa areas between 1995 and 2005, the total annual precipitation change was ($Z = -0.11$ to 0.84), which means the years with lower precipitation than the average. Other regions have relatively low annual precipitation changes ($Z = 0.67$–1.23). There was a decrease in the area's precipitation change until 2010, after which there was an increase ($Z = 0.67$) (Fig. 4).

The Selenge river basin's total annual precipitation data is shown in Table 2, along with Mann–Kendall (MK) estimations, Trend estimations, and slope calculations (Sen's slope).

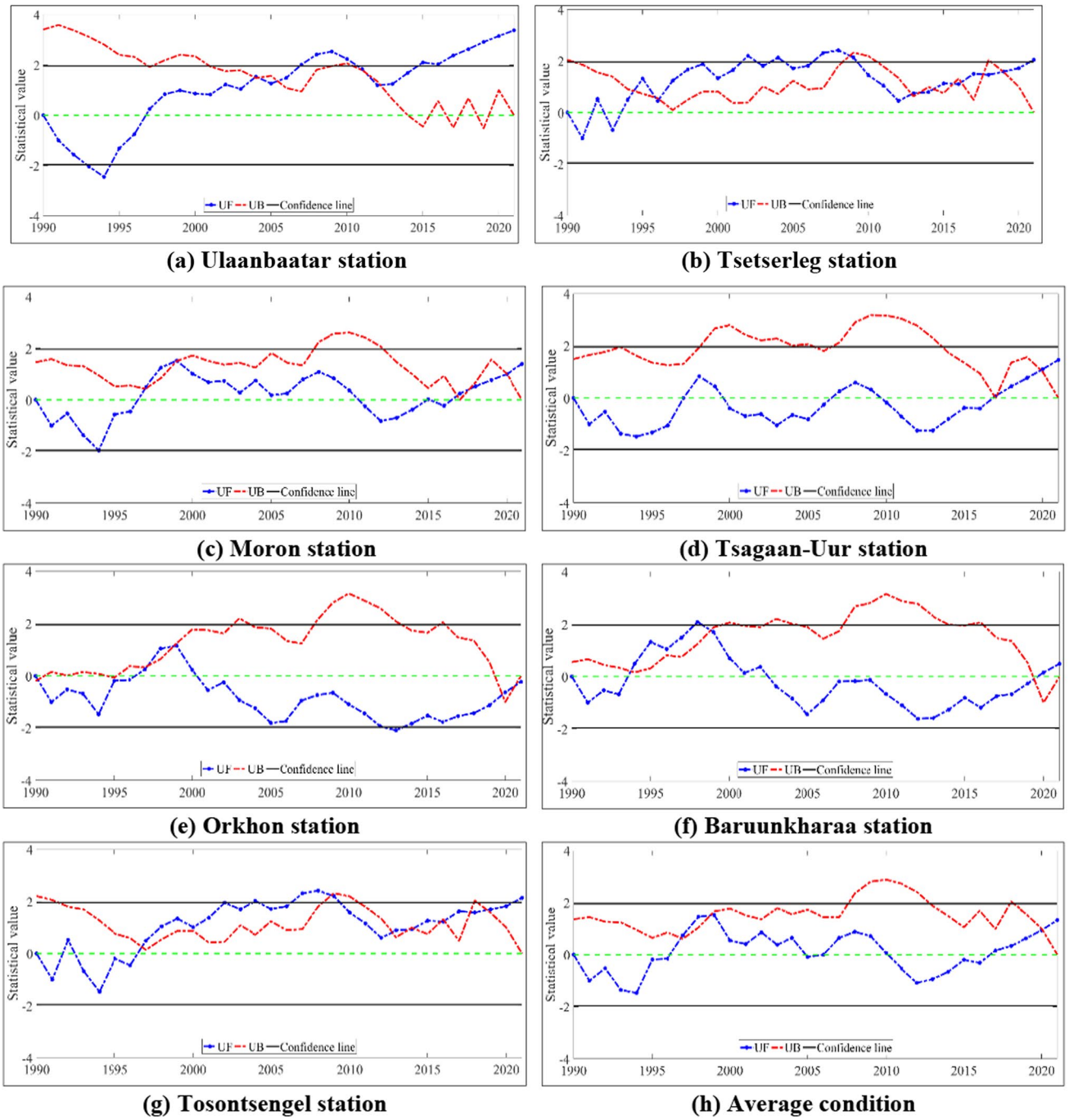

Fig. 3 The long-term trends of annual air temperature

Table 1 A statistical analysis of changes in air temperature along the Selenge River Basin

№	Station name	Z(MK)	Φ(ITAM)	B(SET)
1	Tsetserleg	2.70**	2.70**	0.03
2	Moron	1.88*	9.85***	0.03
3	Tsagaan-Uur	1.95*	– 0.85	0.03
4	Orkhon	– 0.26	– 2.48**	– 0.01
5	Baruunkharaa	0.67	1.26*	0.00
6	Ulaanbaatar	4.50***	-28.86***	0.06
7	Tosontsengel	2.88**	3.46***	0.04
8	Average	1.77*	– 76.25***	0.02

*Trends at 0.1 significance level

**Trends at 0.05 significance level

***Trends at 0.01 significance level

Analysis of River discharge

Using the Mann–Kendall method, we analyzed the average flow data from seven hydrological stations located in the Selenge River basin over the past 31 years. The Eg–Erdenebulgan and Khanui–Erdenemandal hydrological stations exhibit significant changes in average annual flow rates, with Z scores of -3.39 and -3.95, indicating a significant decrease. Even though the average annual flow rate of the Selenge river is between -0.78 and 3.95, a continuous downward trend has been observed in Eg–Erdenebulgan, Khanui–Erdenemandal, and Selenge–Zuunburen since 1992. Since 2015, a slight increase has been observed in the Tuul–Ulaanbaatar, Delgermoron–Moron, and Selenge rivers (Fig. 5).

As shown in Table 3, the average annual flow of the Selenge River basin was calculated using MK, ITAM, and Sen's slope calculation method. According to Mann–Kendall's analysis of river discharges in the basin, all hydrological stations showed a downward trend.

Analysis of land cover

Between 1990 and 2020, Landsat satellite data were used to estimate land cover changes in the Selenge River basin (Table 4). Estimating land cover using satellite data is a highly time and cost-effective process. For this river basin, the maximum-likelihood classification method was applied (Fig. 6).

In the Selenge River basin, land cover changes were assessed across eight classifications. Over the period from 1990 to 2020, the basin witnessed growth in agricultural land, shrubland, wetlands, urban areas, and bare and seasonal snow-ice areas, while forests, grasslands, and water bodies experienced a decrease.

Between 1990 and 2020, spanning the past three decades, changes in the Selenge River basin have primarily been driven by both human activities and natural factors. Human activities have led to an expansion of agricultural land by 6561.0 km^2, an increase in urban area by 335.88 km^2, and an expansion of bare land. Additionally, climate change has acted as a natural influencing factor, resulting in a reduction of water bodies by 63.05 km^2 and a decrease in grassland area by 10,660.7 km^2. Due to the melting of high mountain permafrost and seasonal snow and ice, the area of wetlands has increased by 450.15 km^2 (Table 4, Fig. 7).

Selenge River Basin land cover classification has changed significantly between 1990 and 2020. Thus, a transformation matrix is used to determine which categories of land cover have changed.

A total of 1096.5 km^2 have been converted from bare land to agricultural fields, 31.4 km^2 to forests, 10,466.3 km^2 to pasture, 283.8 km^2 to shrubs, 24.2 km^2 to water bodies, and 138 km^2 to wetlands. In addition, 68.3 km^2 of cultivated land has been converted into bare land, 288.5 km^2 into forests, and 802.1 km^2 into pastures. Forests were converted into 50.7 km^2 of bare land, 612.4 km^2 of cropland, 9167.5 km^2 of grassland, 130.5 km^2 of shrubland, and 43 km^2 of water body. A total of 15,589.3 km^2 of grasslands were converted to bare land, 5361.5 km^2 into cropland, 8721 km^2 into forests, 71.5 km^2 into shrub land, 51.6 km^2 into water bodies, 233.8 km^2 into wetlands. As a result of this research, 389.5 km^2 of shrubland has been converted to bare land, and 9.6 km^2 has been converted to grassland. Approximately 54.1 km^2 of the water body area has been converted to bare land, 32.1 km^2 to forests, 33.7 km^2 to pastures, and 54.5 km^2 to wetlands. Wetland areas of 10.7 km^2 have been converted into bare land, forests of 5.2 km^2, and grasslands of 7.7 km^2 (Table 5). As a result of this study's examination of the accuracy of the 1990–2020 land cover change matrix, a kappa coefficient of 0.81 was obtained. The results of this study indicate that the estimation of land cover changes in the Selenge River basin is accurate and that the interrelationships can be further analyzed.

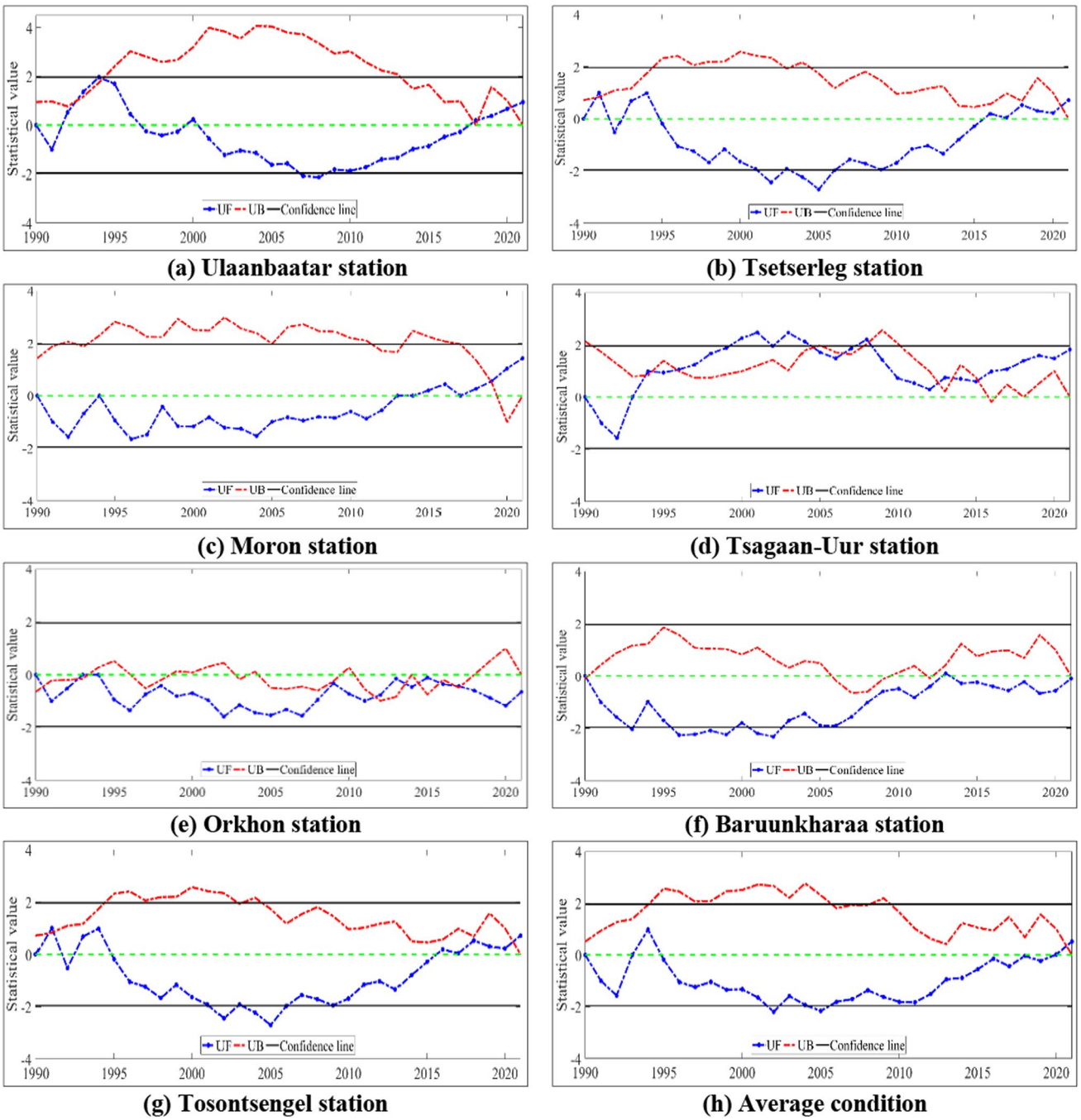

Fig. 4 Long-term trends of precipitation

The relationship between land cover changes, climate change, and river flow

Each year, the average air temperature in the Selenge river basin increases by approximately 0.09 °C. During the last 3 decades, the basin has warmed by 0.5 °C. The warmest year on record was 2007 and the coldest year on record was 2012. The basin's annual average precipitation is 300.2 mm. In recent years, there have been years with lower precipitation than the long-term average in the basin. During the last 3 decades, it has decreased by approximately 0.5 mm per year (Fig. 8). As a result, total annual precipitation has a positive

Table 2 An analysis of precipitation changes in the Selenge River basin based on statistical analysis

№	Station name	Z(MK)	Φ(ITAM)	B(SET)
1	Tsetserleg	0.93	1.16*	1.10*
2	Moron	1.88*	0.87	1.45*
3	Tsagaan-Uur	2.62**	1.16*	4.20***
4	Orkhon	-0.84	0.62	-0.69
5	Baruunkharaa	-0.11	0.67	-0.41
6	Ulaanbaatar	1.23*	0.05	0.97
7	Tosontsengel	0.93	1.15*	1.08*
8	Average	0.67	0.35	0.50

*Trends at 0.1 significance level

**Trends at 0.05 significance level

***Trends at 0.01 significance level

relationship with river flow (r = 0.76, p = 0.0001), precipitation with water bodies ($r = 0.95$, $p = 0.041$), and runoff with water bodies ($r = 0.88$, $p = 0.12$) has a statistically significant high correlation. There is a low correlation between air temperature and other elements ($r = 0.12$, $p = 0.52$), respectively (Fig. 8).

Research conducted in the Selenge River Basin indicates that climate change has a significant impact on land cover change. Examining the temporal and spatial correlations between the main factors influencing climate changes and land cover changes is crucial when it comes to river flows and water resources.

The basin's landscape composition has undergone substantial transformations attributable to both anthropogenic and natural drivers (Table 5, Fig. 9). Notably, Fig. 9a depicts a persistent expansion of cropland within the temporal span from 1990 to 2020. Concurrently, a discernible reduction in river flow within agricultural locales is evident, indicative of escalating water utilization concomitant with agricultural intensification. Moreover, Fig. 9 illustrates a notable decline in discharge at the Tuul–Ulaanbaatar hydrological station since 1995, attributed to a three- to fourfold increase in impervious surface cover and climate change, as depicted in the figure. It is evident that the heightened impervious surfaces have led to a considerable rise in water consumption among the populace. This observed trend underscores the intricate interplay between land surface modifications and hydrological dynamics. Moreover, Fig. 10 illustrates a direct correlation between precipitation patterns in the Selenge River basin and the extent of wetland and water reservoir coverage. Notably, during the period spanning 1990 to 2010, there was a diminution in the area occupied by water bodies categorized within the basin's cover. However, projections based on precipitation and river flow dynamics suggest an anticipated resurgence in water body coverage until 2020, indicative of intricate relationship between climatic variables and basin hydrology.

In terms of land cover change, wetlands, cropland, impervious surfaces, and grasslands have experienced the most significant impacts. Notably, the extent of pasture along the river basin has undergone substantial transformation, assuming various forms. Likewise, cultivated areas, impervious surfaces, and artificial cover have been markedly modified due to human activities. These alterations underscore the shifts in land cover types resulting from human influence. Concurrently, the natural phenomenon of global warming contributes to reduced precipitation and water resources within the basin.

Discussion

An increase in air temperature is a result of changes in the global atmosphere. It has been estimated that the average global temperature has increased by 0.85 °C from 1880 to 2018, and this trend is expected to continue. Since 1985, the water temperature of large water bodies has been increasing rapidly and is 0.045 ± 0.011 °C on average per year (Girma et al. 2023; Li et al. 2023).

Throughout the historical timeline spanning from 1990 to 2020, discernible trends emerge in the average annual air temperature within the Selenge River basin, exhibiting a notable increase of 2.4 °C over the aforementioned period, equating to an average annual increment of 0.09 °C. This escalating thermal regime manifests consequential impacts on the basin's hydrological dynamics, notably influencing total basin-wide evaporation rates (Dorjsuren et al. 2018). Consequently, a discernible reduction in the extent of grassland coverage ensues, juxtaposed by a concomitant expansion in the area characterized by barren land devoid of vegetative cover. These observed shifts underscore the intricate feedback mechanisms between climatic

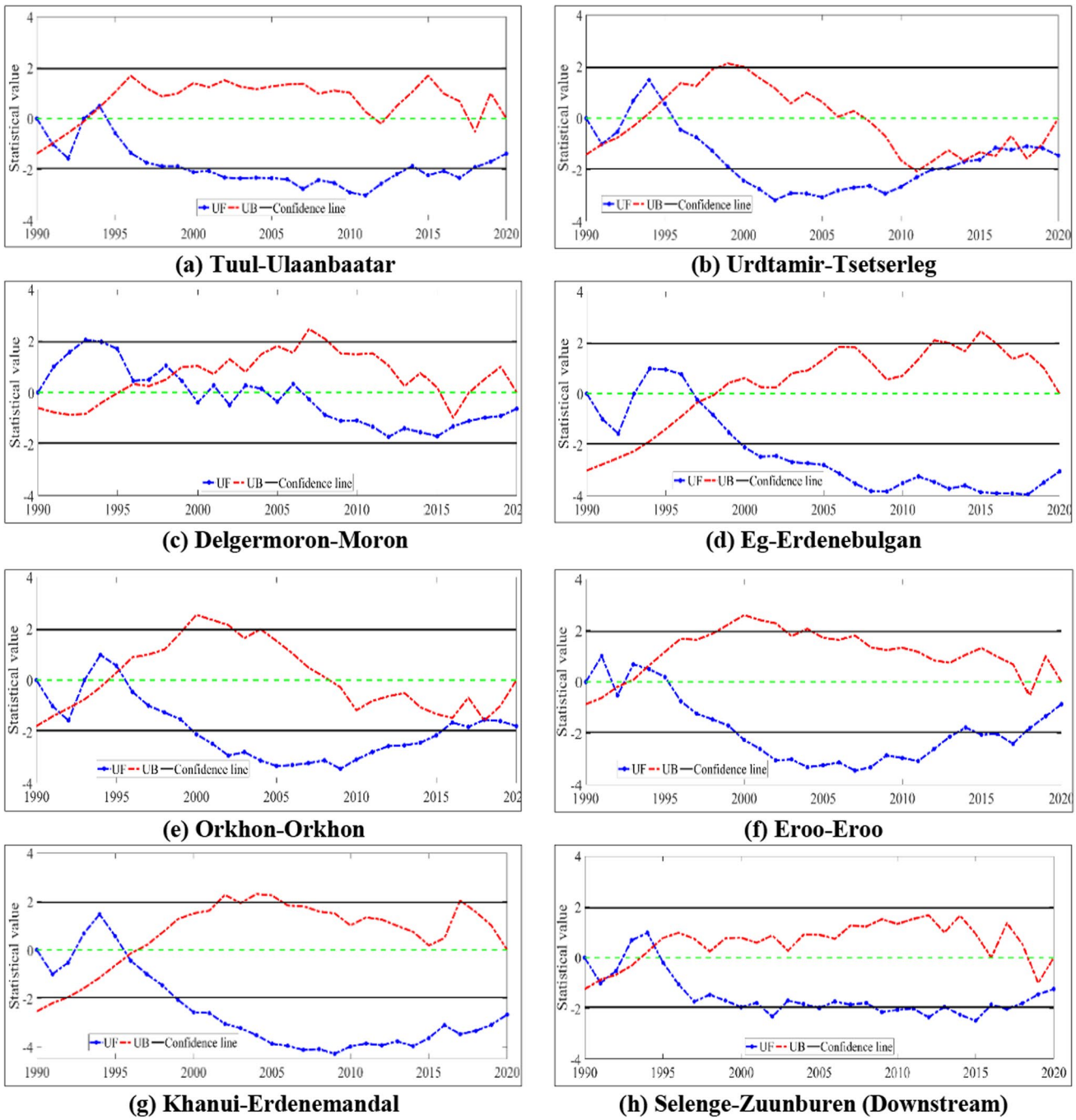

Fig. 5 Long-term trend of River discharge

perturbations and land surface alterations within the basin, underscoring the ecological ramifications of evolving thermal regimes on vegetation dynamics and land cover distributions.

In the mountainous areas of Khangai, Khentii, and Khuvsgul, precipitation averages 300–400 mm per year, whereas in the plains and river valleys, the precipitation averages 150–250 mm per year (Davaa 2015). Generally, the results of this study are consistent with those of other studies, with an increase in temperature and a small change in precipitation (Batima et al. 2005; Dorjsuren et al. 2018). A significant portion of the Selenge River Basin is covered

Table 3 A statistical analysis of Selenge River basin river flow changes

№	Hydrological station	Z(MK)	Φ(ITAM)	B(SET)
1	Delgermoron-Moron	– 0.78	– 1.43*	– 0.21
2	Eg–Erdenebulgan	– 3.95***	– 5.24***	– 0.78
3	Eroo–Eroo	– 1.12*	– 0.50	– 0.25
4	Tuul–Ulaanbaatar	– 1.78*	– 4.61***	– 0.42
5	Orkhon–Orkhon	– 2.32**	– 4.88***	– 0.61
6	Urdtamir–Tsetserleg	– 1.85*	– 2.61**	– 0.11
7	Khanui–Erdenemandal	– 3.39***	– 5.11***	– 0.05
8	Selenge–Zuunburen (Downstream)	– 1.61*	– 1.44*	– 1.72*

*Trends at 0.1 significance level

**Trends at 0.05 significance level

***Trends at 0.01 significance level

by permafrost due to its location in an extreme continental climate zone (Dorjsuren et al. 2018). The Selenge River Basin is characterized by a wide range of stream outlet conditions. In the southern part of the Selenge river basin, soil moisture levels are low, while in the northern part, thick taiga vegetation and permafrost contribute to soil water availability during the summer. Spring water, summer precipitation, and permanent snow are the major sources of the Selenge River basin. Approximately half of the Selenge's annual discharge occurs in the summer (June–August), and groundwater plays a limited role in the river. In the Selenge River basin, runoff is affected by changes in spring runoff and the amount of precipitation during the summer. Between November and March, Selenge river basin rivers have very little flow in winter (3–10% of annual flow), spring snowmelt floods are relatively small, and summer and autumn rain floods are large (Davaa 2015).

Hydrological processes are notably susceptible, especially within the scope of our investigation. Our experimental analysis employing MK, ITAM, and Sen's slope estimator revealed a consistent downward trend in river discharge across all hydrological stations. Since 1995, there has been a pronounced decline in river discharge, likely attributable to the influence of climate change as a natural factor.

In the future, there is a strong need for more detailed studies involving the impacting factors of the changes in land cover and, consequently change of runoff in the Selenge River basin.

Conclusions

The average air temperature of the Selenge river basin has increased by 0.09 °C per year on average, which results in the warming of the climate of the basin by 2.7 °C over the past 30 years. The basin mean annual precipitation has been about 300.2 mm in the last 30 years. Long-term variation of the annual precipitation is relatively low and the annual precipitation amount has been decreasing in recent years.

Table 4 Land cover type and changed area

Land cover type	1990 year		2000 year		2010 year		2020 year	
	km^2	%	km^2	%	km^2	%	km^2	%
Bare land	67,856.25	22.7	70,973.89	23.8	71,246.60	23.8	71,746.31	24.0
Cropland	2361.32	0.79	5798.95	1.94	7051.60	2.36	8274.43	2.77
Forest	90,157.66	30.2	90,555.61	30.3	88,986.74	29.8	89,236.61	29.9
Grassland	133,891.93	44.8	126,526.81	42.4	126,491.38	42.3	124,283.91	41.6
Impervious surface	218.30	0.07	307.29	0.10	412.17	0.14	521.01	0.17
Permanent ice and snow	7.73	0.003	17.06	0.006	15.75	0.005	15.29	0.005
Shrub land	478.68	0.16	574.60	0.19	539.51	0.18	545.43	0.18
Waterbody	3651.77	1.22	3593.09	1.20	3569.70	1.19	3594.94	1.20
Wetland	130.51	0.04	406.84	0.14	440.71	0.15	536.21	0.18
Total area	298,754.14	100.00	298,754.14	100.00	298,754.14	100.00	298,754.14	100.00

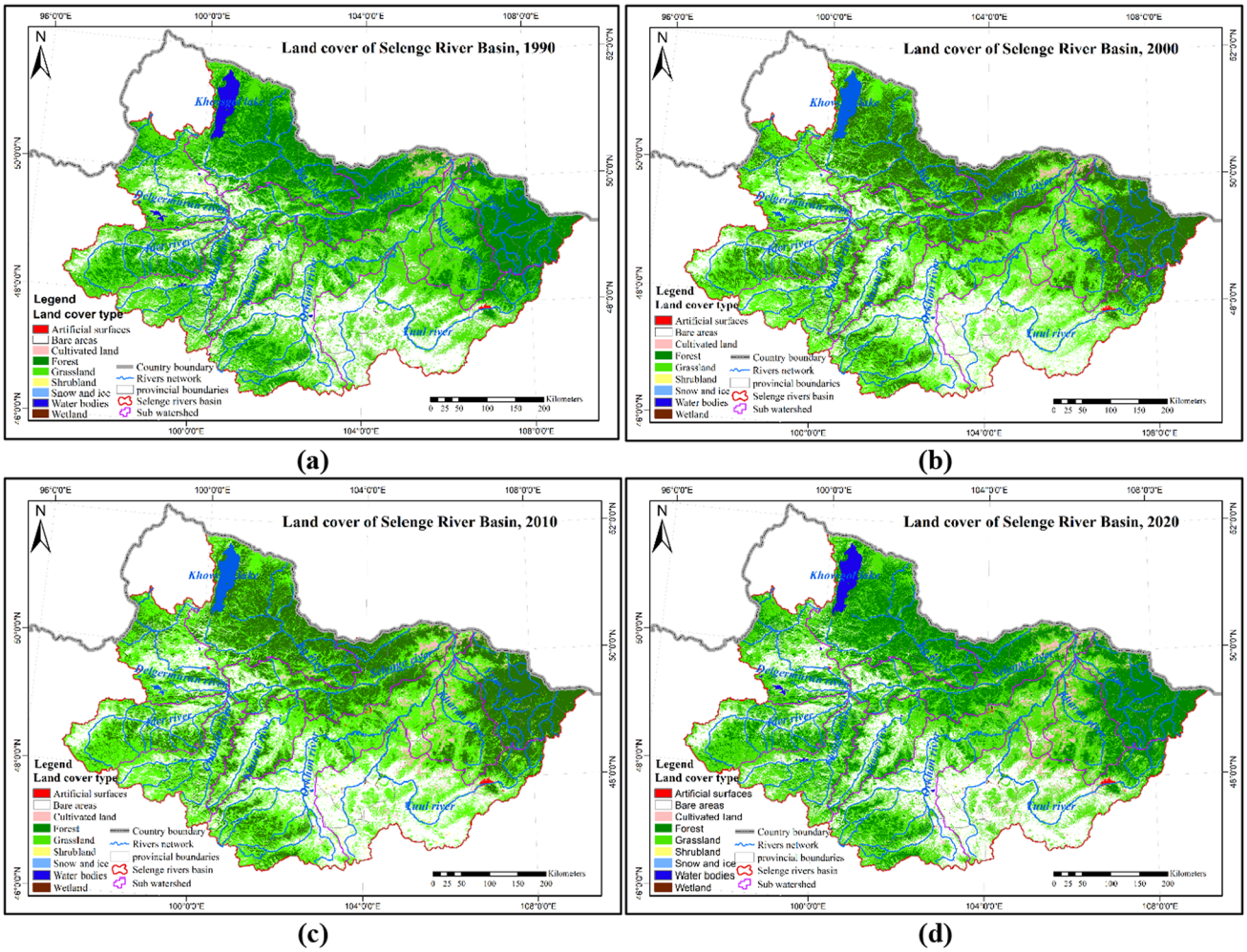

Fig. 6 Land cover changes between 1990 and 2000

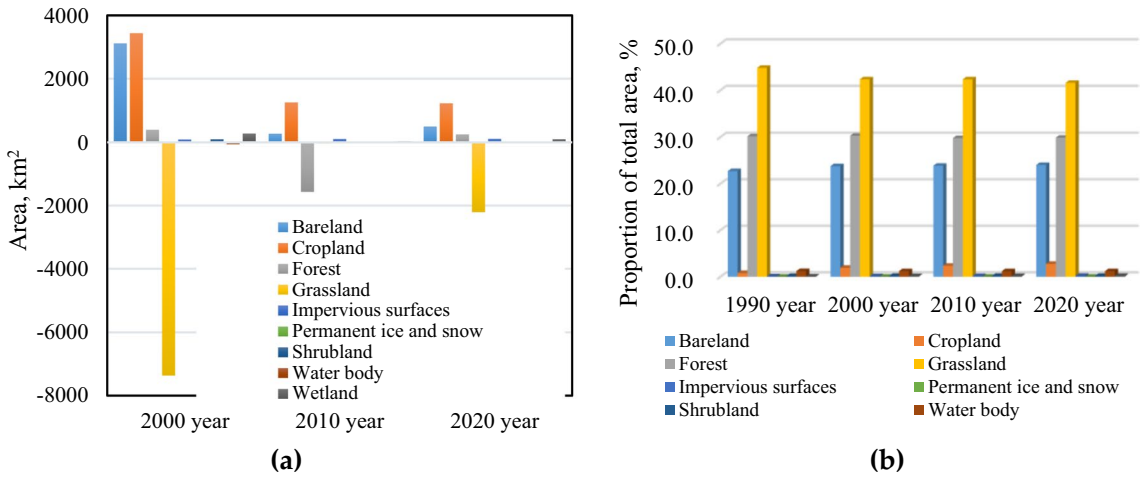

Fig. 7 Land cover changes a) Land cover change between 1990 to 2020. b) Percentage of land cover changes between 1990 to 2020

Table 5 Transition of land cover change (1990–2020)

Land cover types (2020)	Land cover types (1990)								
	Labels	Ba	Cu	Fo	Gr	Si	Sh	Wb	We	Total
	Ba	426.1	68.3	50.7	15,589.3	1.2	389.6	54.1	10.7	16,590.1
	Cu	1,096.5	0.1	621.4	5361.5	0.0	2.9	5.2	1.6	7089.2
	Fo	31.4	288.5	15,245.4	8721.0	0.0	8.3	32.1	5.2	24,331.9
	Gr	10,466.3	802.1	9167.5	0.0	0.0	9.6	33.7	7.7	20,486.9
	Is	164.4	6.1	13.9	109.3	0.0	5.3	3.8	1.2	304.0
	Si	4.9	0.0	0.0	3.2	0.0	0.0	0.2	0.0	8.3
	Sh	283.8	4.6	130.5	71.5	0.0	0.1	0.4	0.1	490.9
	Wb	24.2	4.9	43.0	51.6	0.0	0.1	0.0	2.1	125.9
	We	138.0	9.5	0.0	233.8	0.0	0.8	54.5	0.0	436.7
	Total	12,635.7	1,184.2	25,272.4	30,141.2	1.2	416.6	184.0	28.6	298,754.1

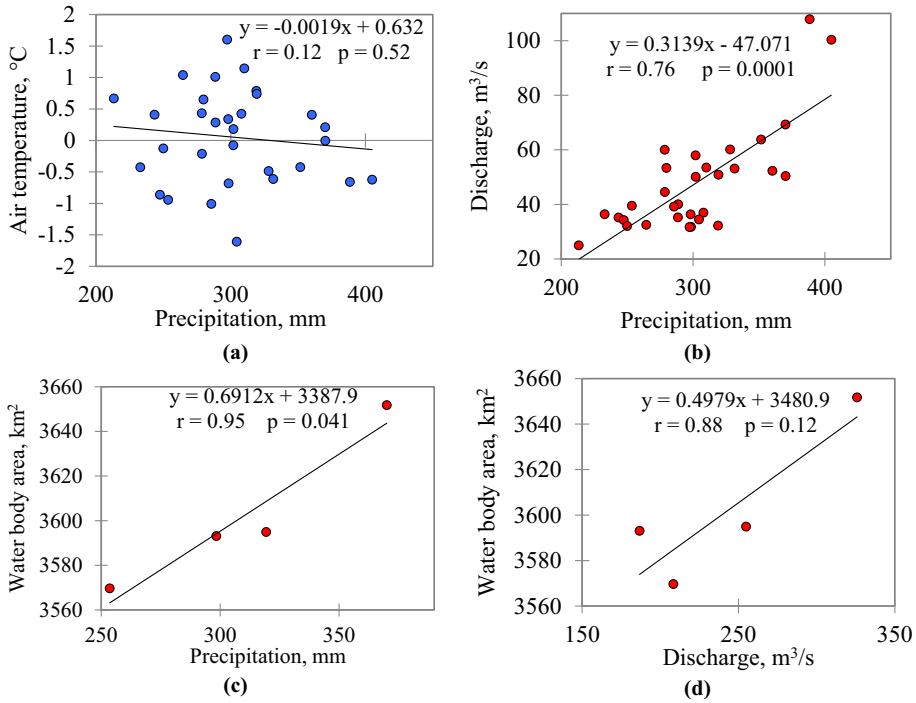

Fig. 8 In the Selenge river basin **a** air temperature and average precipitation in the basin, **b** average precipitation and river flow, **c** precipitation and water bodies, **d** relationship between river flow and water body

The area of water bodies has decreased by 63.05 km^2 and the area of grasslands by 10,660.7 km^2, respectively, in the basin in the last 30 years. The area of cultivated land increased by 6561.0 km^2. The area of the urban regions increased by 335.88 km^2 in the same period. Also, the area without vegetation and wetlands increased by 450.15 km^2.

The research results of our studies also show the kappa coefficient of the matrix of land cover changes in the Selenge River basin in the period 1990–2020 is 0.81 which indicates statistical confidence of our estimation of land cover changes in the Selenge River basin and provides possibilities for further analyze the interrelationship.

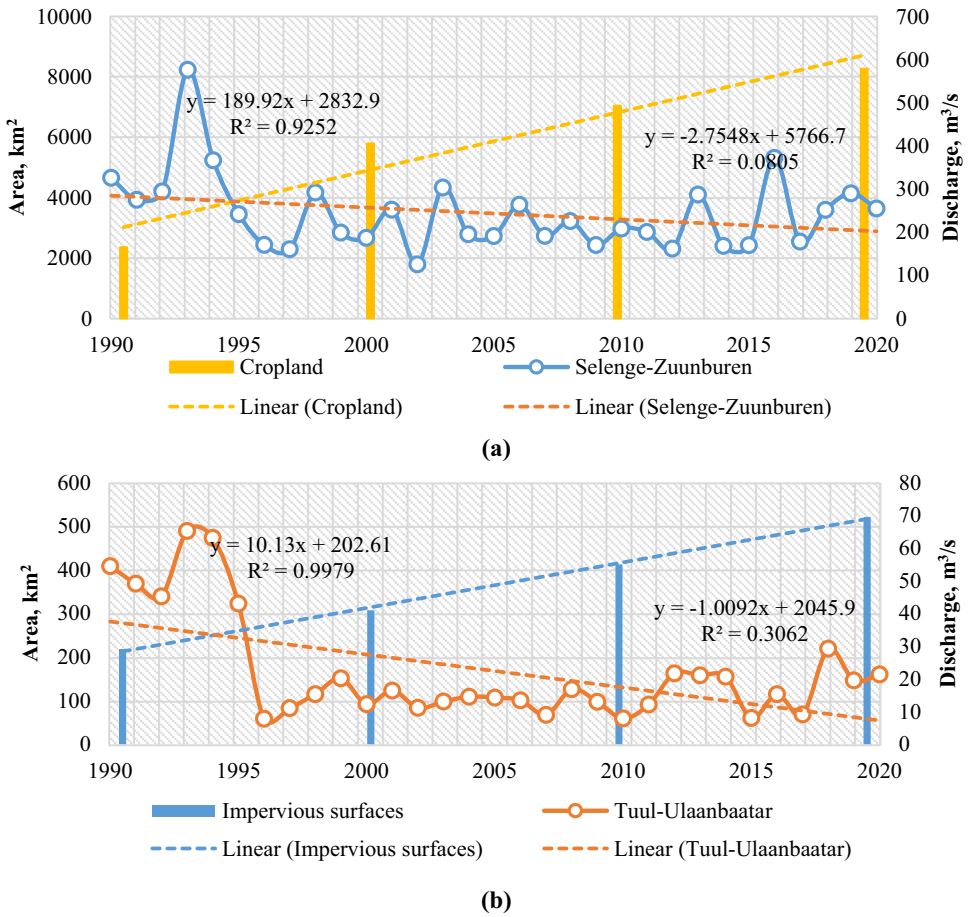

Fig. 9 In the Selenge River Basin, **a** long-term river Selenge–Zonburen flow average runoff and cropland development, **b** long-term river Tuul–Ulaanbaatar flow average runoff and Impervious surfaces development

Total annual precipitation in the Selenge river basin has a positive correlation with river runoff ($r=0.76$, $p=0.0001$), and precipitation and river flow have a statistically significant relationship with the area of water bodies in the basin. ($r=0.88$–0.95, $p=0.041$–0.12) is highly correlated. As for the relationship with air temperature, the correlation was weak with other elements ($r<0.12$, $p=0.52$).

Precipitation and river flow in the basin have decreased to a certain extent, and water bodies and wetlands have changed significantly in the land cover of the basin. Human influences, such as mining, industry, agriculture, and urbanization, have notably increased in recent years in the Selenge River basin.

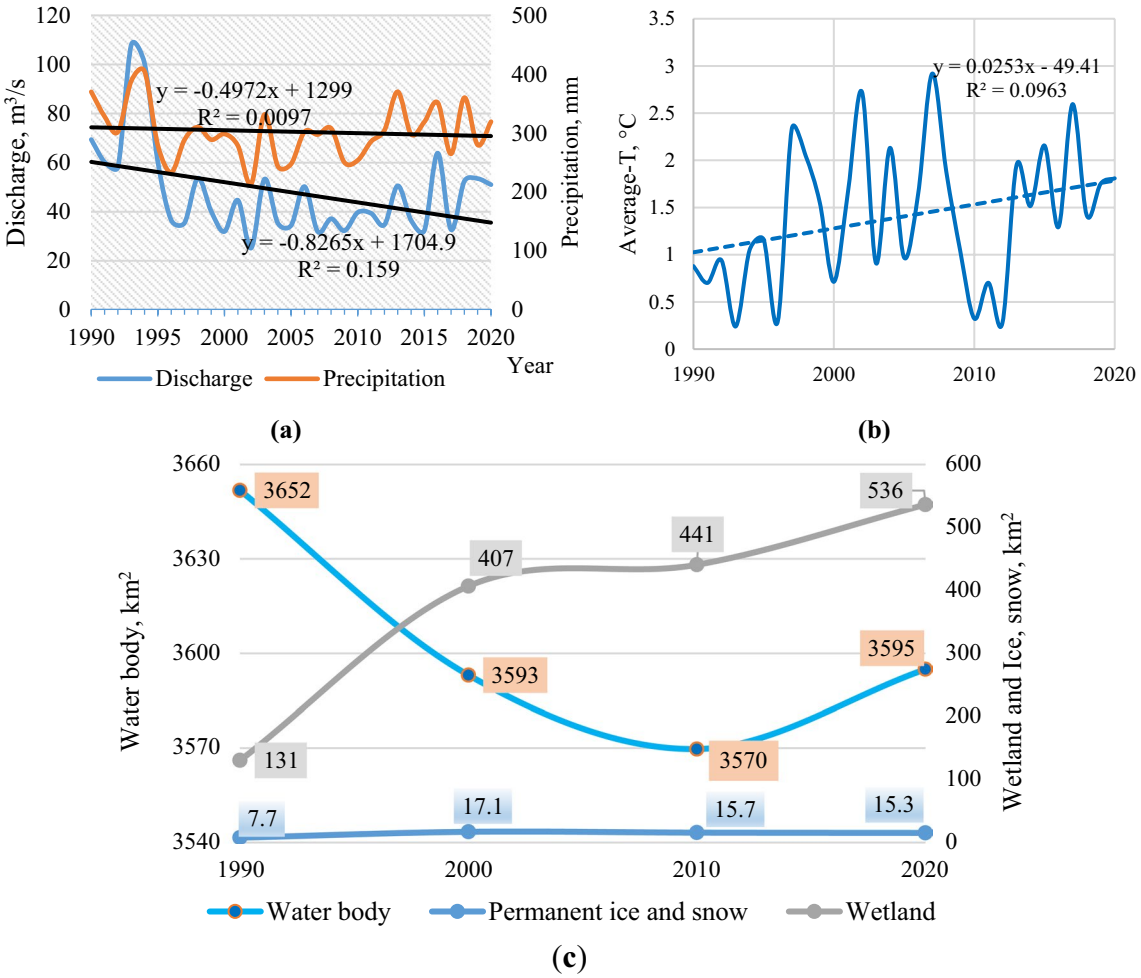

Fig. 10 In the Selenge River Basin, **a** long-term trends of river flow and average precipitation, **b** average air temperature **c** changes in water bodies (1990–2020)

Acknowledgements The authors would like to thank the Information and Research Institute of Meteorology, Hydrology, and Environment of Mongolia for providing the raw meteorological data. Additionally, our appreciation goes to the "Accurate Regulation Method and Coordination Web Platform Development of Animal Husbandry in the Selenge River Basin, Mongolia" project for its financial support of this research.

Author contributions Conceptualization, E.B. and B.D.; methodology, B.D.; software, E.B.; validation, A.O., O.N. and W.J.; formal analysis, E.B.; investigation, B.D.; resources, E.S.; data curation, B.G.; writing original draft preparation, E.B.; writing review and editing, B.D. and A.O.; visualization, A.T.; supervision, B.D.; project administration, A.O.; funding acquisition, W.J. All authors have read and agreed to the published version of the manuscript.

Funding This research was funded by Mongolian Foundation for Science and Technology, grant number NSFC2022/01 and the National Nature Science Foundation of China, grant number 32161143025 and 41971385, Construction Project of the China Knowledge Center for Engineering Sciences and Technology, grant number CKCEST-2023–1-5, Also, supported by the Ministerial Innovation Scholarship for Postdoctoral Research (grant: 19XX04DI208).

Data Availability Not applicable.

Declarations

Conflict of interest The authors declare no conflict of interest.

References

Asfaw A et al (2018) Variability and time series trend analysis of rainfall and temperature in northcentral Ethiopia: A case study in Woleka sub-basin. Weather and Climate Extremes 19:29–41

Batdelger O et al (2022) Spatial and Temporal Isotopic and Hydrochemical Characteristics of Groundwater and Surface Water in the Tuul River Basinm Mongolia. Earth Syst Environ 6(2):517–529

Batima P et al (2005) Observed climate change in Mongolia. Assess Imp Adapt Clim Change Work Pap 12:1–26

Batima P, Bold B, Sainkhuu T, Bavuu M (2008) Adapting to drought, zud and climate change in Mongolia's rangelands. In: Climate change and adaptation, pp 197–210

Cato T et al (2007) *Долдугаар булэг: Урьдчил сан унэлгээ, прогноз.* Зуун хойд Азийн бэлчээрийн агаар-ус-шим мандлын харилцан уилчлэлиин судалгаа (RAISE), туршилт: RAISE теслийн ур дун, 2007. **8**: pp. 66–70.

Chonokhuu S et al (2019) Contamination and health risk assessment of heavy metals in the soil of major cities in Mongolia. Int J Environ Res Public Health 16(14):2552

Cianconi P, Betrò S, Janiri L (2020) The impact of climate change on mental health: a systematic descriptive review. Front Psych 11:74

Cui L et al (2017) Innovative trend analysis of annual and seasonal air temperature and rainfall in the Yangtze River Basin, China during 1960–2015. J Atmos Solar Terr Phys 164:48–59

Davaa G (2015) Surface water regime resource of Mongolia. Ulaanbaatar. Surface Water Regime and Resources of Mongolia is published by the Information and Research Institute of Meteorology, Hydrology and Environment. pp 408

Demberel O et al (2023) Relationship between Dynamics of Modern Glaciers of the Mt. Munkhkhairkhan (Mongolian Altai) and Climate. Water 15(10):1921

Dorjsuren B et al (2018) Observed trends of climate and river discharge in Mongolia's Selenga sub-basin of the lake Baikal basin. Water 10(10):1436. https://doi.org/10.3390/w10101436

Dorjsuren B, Yan D, Wang H, Chonokhuu S, Enkhbold A, Yiran X, Girma A, Gedefaw M, Abiyu A (2018) Observed trends of climate and land cover changes in Lake Baikal basin. Water10:1436. https://doi.org/10.3390/w10101436

Dorjsuren B, Batsaikhan N, Yan D, Yadamjav O, Chonokhuu S, Enkhbold A, Qin T, Weng B, Bi W, Demberel O, Boldsaikhan T (2021) Study on relationship of land cover changes and ecohydrological processes of the Tuul River Basin. Sustainability 13:1153. https://doi.org/10.3390/su13031153

Enkhbold A et al (2022) Impact of faults on the origin of lake depressions: a case study of Bayan Nuur depression, North-west Mongolia, Central Asia. Geogr Fis Din Quat 44:69–82

Erdenejargal N et al (2021) Evaluation of the natural landscape aesthetic: a case study of Uvs province, Mongolia. Pol J Environ Stud 30(5):4497–4509

Førland EJ, Benestad R, Hanssen-Bauer I, Haugen JE, Skaugen TE (2011) Temperature and precipitation development at Svalbard 1900–2100. Adv Meteorol 1–14

Gedefaw M et al (2018a) Innovative trend analysis of annual and seasonal rainfall variability in Amhara regional state ethiopia. Atmosphere 9(9):326

Gedefaw M et al (2018b) Trend analysis of climatic and hydrological variables in the Awash river basin ethiopia. Water 10(11):1554

Girma A et al (2023) Climate change, land use, and vegetation evolution in the Upper Huai River Basin. Atmosphere 14(3):512

Hansen J et al (2001) A closer look at United States and global surface temperature change. J Geophys Res Atmos 106(D20):23947–23963

Karthe D et al (2017) Assessment of runoff, water and sediment quality in the Selenga River basin aided by a web-based geoservice. Water Resour 44:399–416

Konya K et al (2013) Surface mass balance of the Potanin Glacier in the Mongolian Altai Mountains and comparison with Russian Altai glaciers in 2005, 2008, and 2009. Bull Glaciol Res 31:9–18

Li J et al (2023) Estimating effects of natural and anthropogenic activities on trophic level of inland water: analysis of Poyang Lake Basin, China, with Landsat-8 observations. Remote Sens 15(6):1618

Ma X et al (2003) Hydrological regime analysis of the Selenge River basin Mongolia. Hydrol Process 17(14):2929–2945

Ma X et al (2014) Spatial and temporal variation in rainfall erosivity in a Himalayan watershed. CATENA 121:248–259

Masson-Delmotte V, Zhai P, Pirani A, Connors SL, Péan C, Berger S, Caud N, Chen Y, Goldfarb L, Gomis M (2021) Climate change 2021: the physical science basis. In: Contribution of working group I to the sixth assessment report of the intergovernmental panel on climate change, p 2

McClelland JW, Déry SJ, Peterson BJ, Holmes RM, Wood EF (2006) A pan-arctic evaluation of changes in river discharge during the latter half of the 20th century. Geophys Res Lett 33(6). https://doi.org/10.1029/2006GL025753

McCright AM, Dunlap RE, Xiao C (2013) Perceived scientific agreement and support for government action on climate change in the USA. Clim Change 119(2):511–518

Millar RJ et al (2017) Emission budgets and pathways consistent with limiting warming to 1.5 C. Nat Geosci 10(10):741–747

Ren Y et al (2022) Comparative analysis of driving forces of land use/cover change in the upper, middle and lower reaches of the Selenga River Basin. Land Use Policy 117:106118

Sato K et al (2007) Critical role of ABCA1 transporter in sphingosine 1-phosphate release from astrocytes. J Neurochem 103(6):2610–2619

Sato T et al (2008) Functional analysis of JAK3 mutations in transient myeloproliferative disorder and acute megakaryoblastic leukaemia accompanying Down syndrome. Br J Hematol 141(5):681–688

Stubblefield A et al (2005) Impacts of gold mining and land use alterations on the water quality of central Mongolian rivers. Integr Environ Assess Manag Int J 1(4):365–373

Timofeev IV, Kosheleva NE (2017) Geochemical disturbance of soil cover in the nonferrous mining centers of the Selenga River basin. Environ Geochem Health 39(4):803–819

Wu H, Qian H (2017) Innovative trend analysis of annual and seasonal rainfall and extreme values in Shaanxi, China, since the 1950s. Int J Climatol 37(5):2582–2592

Wu H, Liu DF, Chang JX, Zhang HX, Huang Q (2017) Impacts of climate change and human activities on runoff in Weihe Basin based on Budyko hypothesis. IOP Conf Ser Earth Environ Sci 82:012063. https://doi.org/10.1088/1755-1315/82/1/012063

Yembuu B (2021) Climate and climate change of Mongolia. In: Yembuu B (ed) The physical geography of Mongolia. Springer International Publishing, Cham, pp 51–76

Zorigt M et al (2019) Runoff dynamics of the upper Selenge basin, a major water source for Lake Baikal, under a warming climate. Reg Environ Change 19(8):2609–2619

Гармаев ЕЖ, Доржготов Д (2010) Изменение климата и сток рек Байкальского региона. Вестник Бурятского Государственного Университета Биология География 4:17–20

Цыренова, ТБ (2011) *Государственное управление водными ресурсами в условиях межгосударственного взаимодействия России и Монголии*. 2011, Забайкальский государственный университет.

Authors and Affiliations

Erdenebayar Bavuu[1,2] · Batsuren Dorjsuren[1,5] · Davaa Gombo[2] · Juanle Wang[3] · Erdenetsetseg Sugar[1] · Bolorjargal Ganzorig[2] · Oyunchimeg Namsrai[1] · Adiyasuren Tserenjargal[4] · Shuxing Xu[3] · Yating Shao[3] · Altansukh Ochir[1]

✉ Batsuren Dorjsuren
batsuren@seas.num.edu.mn; batsuren@num.edu.mn

Erdenebayar Bavuu
erdenebayar@irimhe.namem.gov.mn

Davaa Gombo
watersect@yahoo.com

Juanle Wang
wangjl@igsnrr.ac.cn

Erdenetsetseg Sugar
erdenetsetseg@met.gov.mn

Bolorjargal Ganzorig
bolorjargal@irimhe.namem.gov.mn

Oyunchimeg Namsrai
n.oyunchimeg@num.edu.mn

Adiyasuren Tserenjargal
adiyasuren_ts@namem.gov.mn

Shuxing Xu
xusx@lreis.ac.cn

Yating Shao
shaoyt@lreis.ac.cn

Altansukh Ochir
altansukh@num.edu.mn

[1] Environmental Engineering Laboratory, Department of Environment and Forest Engineering, School of Engineering and Technology, National University of Mongolia, Ulaanbaatar 14201, Mongolia

[2] Hydrology Division, The Information and Research Institute of Meteorology, Hydrology and Environment (IRIMHE), Ulaanbaatar 15160, Mongolia

[3] State Key Laboratory of Resources and Environmental Information System, Institute of Geographic Sciences and Natural Resources Research, Chinese Academy of Sciences, Datun Road A11, Chaoyang District, Beijing 100101, China

[4] Division of Observation Network and Climate, National Agency of Meteorology and Environmental Monitoring, Ulaanbaatar 15160, Mongolia

[5] Department of Hydrology, National Research Tomsk State University, Tomsk 634050, Russia